Assessment of elastin and collagen contribution to aortic elasticity in conscious dogs

RICARDO LUIS ARMENTANO, JAIME LEVENSON, JUAN GABRIEL BARRA, EDMUNDO IGNACIO CABRERA FISCHER, GUSTAVO JAVIER BREITBART, RICARDO HORACIO PICHEL, AND ALAIN SIMON
Research and Teaching Department, Favaloro Foundation, 1078 Buenos Aires, Argentina; and Institut National de la Santé et de la Recherche Médicale U28, Centre de Diagnostic, Hôpital Broussais, 75674 Paris, Cedex 14, France

ARMENTANO, RICARDO LUIS, JAIME LEVENSON, JUAN GABRIEL BARRA, EDMUNDO IGNACIO CABRERA FISCHER, GUSTAVO JAVIER BREITBART, RICARDO HORACIO PICHEL, AND ALAIN SIMON. *Assessment of elastin and collagen contribution to aortic elasticity in conscious dogs.* Am. J. Physiol. 260 (Heart Circ. Physiol. 29): H1870–H1877, 1991.—The elastic behavior of total elastin (E_E) and collagen (E_C) and the recruitment of collagen fibers (FC) supporting wall stress at a given transmural pressure level were assessed in seven conscious dogs using descending thoracic aortic pressure (microtransducer) and diameter (sonomicrometer) measurements. Stress-strain relationships values calculated at control and during bolus administration of angiotensin and nitroglycerin enabled quantification of elastic moduli of elastin ($E_E = 4.868 \pm 1.753 \times 10^6$ dyn/cm^2; means ± SD) and collagen ($E_C = 1{,}306 \pm 637 \times 10^6$ dyn/cm^2) according to a biphasic model of elastin and collagen parallel arrangement. The FC was found to be 6.1 ± 2.6% at a pressure level of 118 ± 16 mmHg. Values for E_E and E_C were similar to those reported in in vitro studies and showed scarce variability. This approach provides a quantitative evaluation of elastin and collagen moduli in conscious animals and also permits the evaluation of FC, which may be of interest in studies of connective tissue diseases involving the aortic wall.

Young's modulus; aortic properties; stress-strain relationship; collagen recruitment function

THE MECHANICAL PROPERTIES of the aortic wall play a major role in the regulation of the relationship between aortic pressure and diameter (22) as well as in the determination of the degree of wall stress and compression of the baroreceptors within the wall (25). The elastic behavior of blood vessels is usually studied using linear elastic theory. However, the nonlinearity of the stress-strain relationship and the anisotropy of the wall (7, 34) represent major constraints in the use of the linear analysis. For a better description of the elastic behavior of the arterial wall, it would be necessary to take into account the relative contributions of the different components of the vessel to the overall elastic modulus. The participation of collagen and elastin in the mechanical properties has been widely studied in in vitro preparations (8, 13, 14, 21, 31, 32). These studies indicate that the values of Young's modulus are strongly different for elastin and collagen (3, 14, 16, 20, 24). In addition, a recruitment function for collagen fibers (FC) was described in vitro in terms of the fraction of total collagen fibers supporting wall stress at a given transmural pressure (3, 9, 11). This function shows a nonlinear behavior. However, to our knowledge, no study regarding the assessment of the individual elastic moduli of the connective tissue components of the arterial wall and the recruitment function of the collagen has been reported in conscious animals.

Using the stress-strain relationship in the thoracic aortas of chronically instrumented dogs, we present an original method for the resolution of Young's modulus into its elastin and collagen components in chronically instrumented conscious dogs. This method also enables us to obtain a FC representing the degree of involvement of collagen fibers in the support of load on the aortic wall.

MATERIALS AND METHODS

Surgical Preparation

Seven male mongrel dogs aged 54.9 ± 8.8 mo and weighing 20.4 ± 1.8 kg were prepared for this study. On arrival at the animal house, the dogs were vaccinated against rabies, distemper, hepatitis, parvovirus, and leptospirosis, and were treated for skin and intestinal parasites. For 20 days before surgery, they were appropriately fed and watered and were assessed for adequate clinical status.

Anesthesia was induced with intravenous thiopental sodium (20 mg/kg), and, after intubation, anesthesia was maintained with 2.5% enflurane carried in pure oxygen (4 l/min) through a Bain tube connected to a Bird Mark VIII respirator. A sterile thoracotomy was made at the left fourth intercostal space. A pressure microtransducer (Konigsberg P7, 1,200 Hz frequency response) and a fluid-filled polyvinyl chloride catheter (2.8 mm OD, for later calibration of the microtransducer) were implanted in the descending thoracic aorta through a stab wound in the left brachial artery. A pair of ultrasonic crystals (5 MHz, 4 mm diam) was sutured on the adventitia of the aorta, after minimal dissection, to measure external aortic diameter. The transit time of the ultrasonic signal (1,580 m/s) was converted into distance using a sonomicrometer (Triton Technology, 100-Hz frequency re-

sponse) and was observed on the screen of an oscilloscope (Tektronix 465B) to confirm optimal signal quality. A polyvinyl chloride catheter (2.3 mm OD) was advanced through the left mammary vein to lie in the superior vena cava or right atrium for drug administration. A hydraulic cuff occluder made from silicon rubber was implanted around the descending thoracic aorta through a second thoracotomy performed at the left seventh intercostal space (Fig. 1). Before the thoracotomies were repaired, all cables and catheters were tunneled subcutaneously to emerge at the interscapular space. All animals were allowed to recover under veterinary care. Ampicillin (20 $mg \cdot kg^{-1} \cdot day^{-1}$ im) was given for a period of 7 days after surgery. The catheters were flushed daily with heparinized saline.

Experimental Protocol

Experiments were performed starting on the seventh postoperative day. At this time, the dogs had completely recovered from surgery, were active, eating well, and were free of any apparent signs of infection. Each study was performed with the dog resting quietly on its right side in the conscious, unsedated state.

The aortic pressure was determined using the pressure microtransducer, which had been calibrated against a Statham-P23 transducer connected to the aortic fluid-filled catheter. The zero reference point was set at the level of the right atrium. The Statham P23 transducer was previously calibrated using a mercury manometer. The external aortic diameter signal was first centered in the recorder channel and then calibrated in millimeters using the step calibration facility of the sonomicrometer.

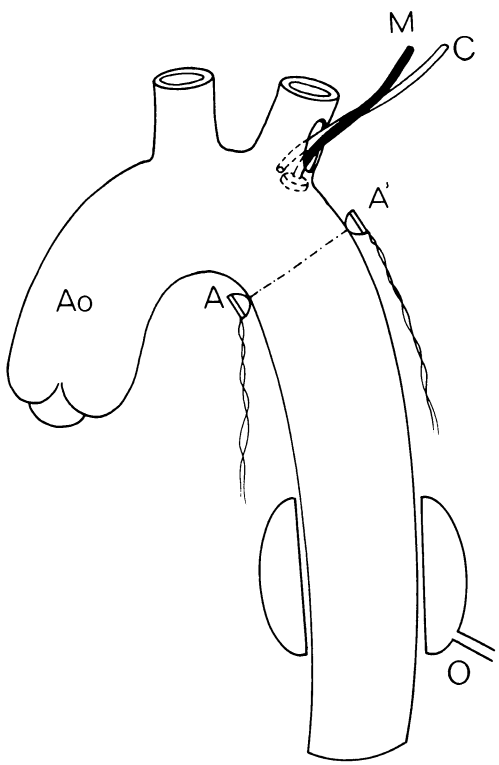

FIG. 1. Schematic representation of animal preparation. Ao, aorta; M, pressure microtransducer; C, fluid-filled catheter; A-A', external diameter crystals; O, aortic cuff occluder.

Aortic pressure and diameter signals were stored on an FM tape recorder (Hewlett-Packard 3968-A) for later digital analysis and were also registered on a six-channel chart recorder (Gould 2600) and displayed on the screen of a four-channel monitor (Gould 51–2341). Instantaneous pressure-diameter loops were displayed on-line on a computer (Apple-II-Plus) using a multichannel 12-bit analog-to-digital converter (AI-13). A specific program, developed in our laboratory (12), was modified for this purpose.

A 5% dextrose drip was started through the mammary vein catheter. In each experimental session, aortic pressure and external diameter were recorded and stored under basal conditions, during an intravenous angiotensin bolus (0.1 μg/kg), and during an intravenous bolus of nitroglycerin (25 μg/kg). The angiotensin and nitroglycerin boluses were administered to obtain a wide range of pressure-diameter relationships. Ten minutes were allowed to elapse between these interventions to return to basal values. Occlusions of the descending thoracic aorta were also performed by means of the aortic cuff occluder.

In four dogs, the experimental session was repeated on the 10th and 13th postoperative days to make the variability study. On the day after the final experimental session, the dogs were killed with an intravenous overdose of thiopental sodium followed by potassium chloride. The correct positioning of the dimension gauges in all dogs was verified at autopsy.

Data Collection

Aortic pressure and diameter signals were sampled and analyzed off-line on an IBM-XT computer, equipped with a Data Translation 2801-A analog-to-digital converter. Signals were digitized every 5 ms during control resting condition and during the transient state after the angiotensin and the nitroglycerin boluses. Approximately 20 consecutive beats during the control resting condition were averaged to obtain mean, systolic, diastolic, and pulse aortic pressures and diameters, and heart rate.

During the transient state all beats were digitized, starting from the beat before the onset of variation of the pressure and diameter signals until the beat before the maximal effect produced by each drug. Moreover, to evaluate the collagen elastic modulus, the beats corresponding to the steady state immediately after the angiotensin bolus, including the maximal effect obtained in the maneuver, were acquired.

The procedure to determine the elastic behavior of total elastin (E_E) and collagen (E_C) in the transient state was performed using specially developed programs in the ASYST language (Macmillan Software).

Aortic wall thickness (h) was calculated as the difference between the external aortic radius (r_e) and the internal aortic radius (r_i). To estimate r_i, the following equation was used

$$r_i = [r_e^2 - (V/\pi L)]^{0.5}$$

where V is volume and L is the length of a given aortic wall segment. This segment of thoracic descending aorta

(25–30 mm) adjacent to the dimension gauges was marked with two sutures, and the distance between them was measured during surgery using a caliper. This segment was then carefully dissected free from surrounding tissue, cut at the markers, and weighed on a precision balance (Sartorius-Werke type 2442, FRG). V was calculated using the weight of the aortic wall segment and assuming a tissue density of 1.066 g/ml. Because V does not change in vivo, values of r_i and thus h can be calculated on a continuous basis (13).

Stress (σ) was assessed using a linear elastic theory and assuming an isotropic homogeneous elastic material for the aortic wall, according to the following equation (27, 35)

$$\sigma = \frac{2P(r_e \cdot r_i)^2}{r_e^2 - r_i^2} \cdot \frac{1}{R^2}$$

where P is aortic pressure, and $R = (r_e + r_i)/2$ is the midwall radius.

Strain (ϵ) was obtained from the ratio of R and the minimum midwall radius observed during each experimental session

$$\epsilon = R/R_{min}$$

The pressure-strain elastic modulus (E_P) was calculated as the pulse pressure multiplied by the mean diameter and divided by the pulsatile change in diameter (24).

Calculations

Using a simple model of collagen and elastin fibers arranged in parallel, Cox (9) showed that differences in the passive mechanical properties might be due to differences in the proportion of collagen fibers supporting wall stress at different pressures. Based on this hypothesis, the elastic modulus of the arterial wall is represented by

$$E = E_e \cdot W_e + E_c \cdot W_c \cdot FC \quad (1)$$

where E_e and E_c are the elastic moduli of elastin and collagen respectively, W_e and W_c are the relative amounts of elastin and collagen in the aortic wall, respectively, and FC is the proportion of collagen fibers supporting wall stress at a given strain. With this approach the stress-strain relationship can be written as

$$\sigma = E_e \cdot W_e(\epsilon - \epsilon_{0E}) + E_c \cdot W_c \cdot FC \cdot \epsilon \quad (2)$$

where ϵ_{0E} is the strain axis intercept, i.e., the extrapolated value of strain for stress equal to zero.

E_E. Because at low pressure the resistance to stretch is due to elastin alone (32), the first part of the stress-strain relationship shows a linear behavior (Fig. 2*A*). Beyond a certain value of stress that we call the "breakpoint," the stress-strain relationship follows an upward curve as collagen fibers are recruited. This breakpoint is detected as the last point before which the extrapolated linear function emerges from the nonlinear stress-strain relationships. Below this critical point, the linear response of the aortic wall can be fitted with a linear model in which $E_e \cdot W_e$ is the slope of the linear relation (Fig. 2*B*). Therefore, the stress-strain relationship for this linear portion can be written as

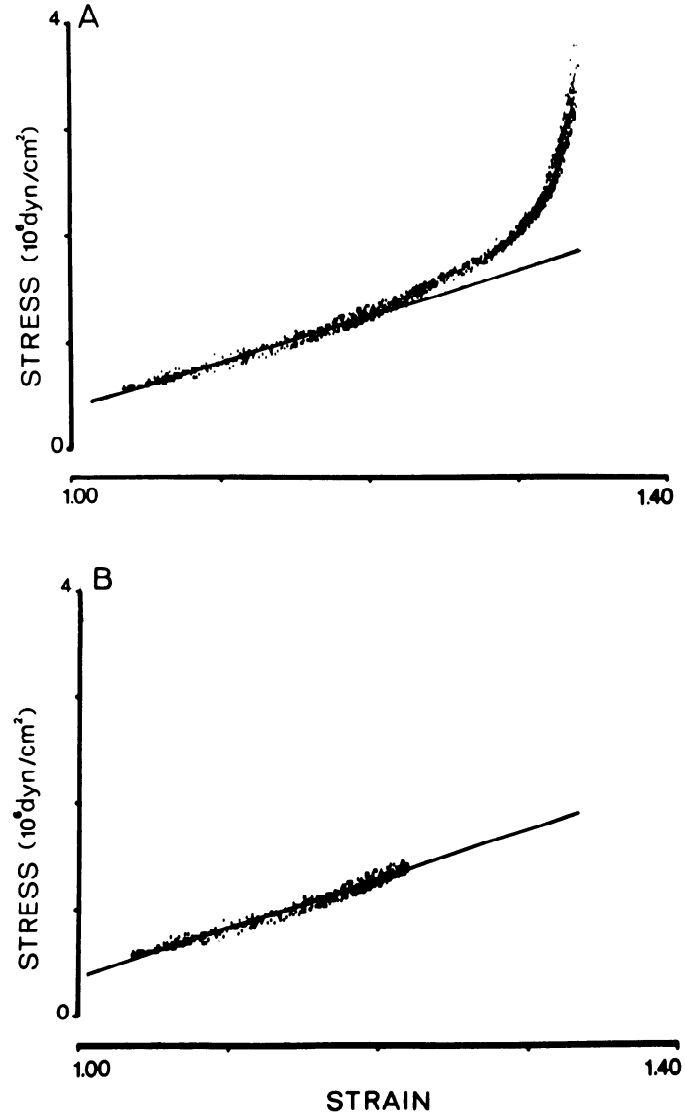

FIG. 2. Determination of elasticity of elastin fibers due to stretch. *A*: aortic stress-strain relationship in a typical dog obtained pharmacologically by boluses of angiotensin and nitroglycerin. *B*: aortic stress-strain points determining elasticity of elastin fibers. Superimposed is corresponding linear regression line.

$$\sigma_E = E_e \cdot W_e(\epsilon - \epsilon_{0E}) \quad (3)$$

where $E_e \cdot W_e$ expresses the E_E. Hence

$$E_E = E_e \cdot W_e \quad (4)$$

E_C. To describe the E_C, it is necessary to separate the stress-strain relationship corresponding to elastin from the overall stress-strain relationship. According to this approach, the collagen behavior is given by the following relation

$$\sigma_C = \sigma - \sigma_E = E_c \cdot W_c \cdot FC \cdot \epsilon \quad (5)$$

where $E_c \cdot W_c$ expresses the E_C. Consequently

$$E_C = E_c \cdot W_c \quad (6)$$

To obtain E_C it is necessary to calculate the difference between the values obtained using *Eqs. 2* and *3* at each strain value (Fig. 3*A*). It can be seen (*Eq. 5*) that the

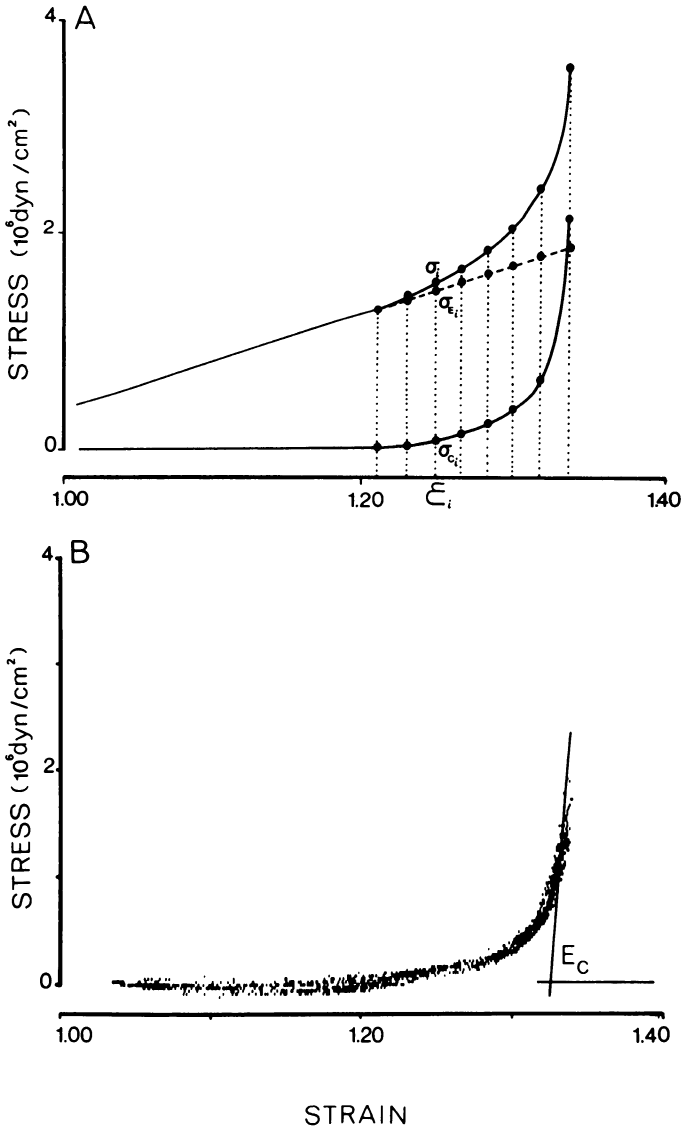

FIG. 3. Determination of elasticity of collagen fibers. *A*: nonlinear function depicted on graph is entire aortic stress-strain relationship. Calculated linear function (dashed line) emerging from nonlinear function shows elasticity of elastin fibers. Points obtained by subtracting values of linear function ($\sigma_{E,i}$) from the entire nonlinear function (σ_i) at any value of strain (ϵ_i) determine a new function ($\sigma_{C,i}$, solid curve on the graph). *B*: collagen stress-strain relationship obtained with procedure described in *A* using same data as in Fig. 1. Elastic modulus of collagen fibers is represented by slope at final portion of curve (solid line).

stress-strain relationship (Fig. 3*B*) is determined by $E_c \cdot W_c$ and FC and represents the resistance to stretch due to both the stiffness and the organization of the collagen fibers. At high stress levels it may be assumed that the normalized FC is close to unity, and then E_C would be calculated as the final slope of the collagen stress-strain relationship.

FC. With the value corresponding to E_C and the stress-strain relationship for the collagen fibers, FC was calculated as

$$FC = \sigma_C/(\epsilon \cdot E_C) \quad (7)$$

At low levels of transmural pressure, FC approaches zero, because no collagen fibers are supporting wall stress (32). Normalization of FC was performed considering a value of 100% as the point of maximum observed stress. At this stress level, it is assumed that all the collagen fibers supporting load on the aortic wall are recruited.

Statistical Analysis

All measurements and calculated values are expressed as means ± SD. Linear regression was analyzed using the least-squares method. To evaluate the variability in each parameter, a coefficient of variation defined as (SD/mean) × 100 was calculated and expressed as a percentage from three experimental sessions in each dog. Day-to-day repeatability in each parameter was studied using a repeated measures one-way analysis of variance (ANOVA). The presence of significant differences was assessed using a paired *t* test or post hoc test after ANOVA. Values of *P* or *F* ratio <0.05 were considered statistically significant (36).

RESULTS

Table 1 shows the group baseline values for systolic, diastolic, and mean aortic pressures and diameters, and heart rate. Table 2 shows the changes in pressure and diameter obtained after maneuvers. Significant increases ($P < 0.05$) in systolic pressure and diameter with respect to systolic basal values were produced by the angiotensin bolus. The maximum pressure observed during the second phase of the angiotensin bolus was 231.06 ± 35.60 mmHg. The nitroglycerin bolus produced significant decreases ($P < 0.05$) in diastolic pressure and diameter with respect to diastolic basal values.

The pressure-diameter relationships obtained pharmacologically by the angiotensin bolus and by occlusion of the implanted aortic occluder were virtually identical as can be seen in Fig. 4.

The use of a linear mathematical model to characterize the elastic response of the elastin fibers is supported by the high linear correlation coefficients (0.972 ± 0.022, $P < 0.0001$) found in the analysis of the first portion of the

TABLE 1. *Basal hemodynamic state*

Basal Hemodynamic State	
Aortic systolic pressure, mmHg	130.80±13.70
Aortic diastolic pressure, mmHg	79.58±14.65
Aortic mean pressure, mmHg	104.47±13.48
Aortic systolic diam, mm	16.94±1.69
Aortic diastolic diam, mm	15.20±1.40
Aortic mean diam, mm	16.22±1.50
Heart rate, beats/min	104.50±15.99

Values are means ± SD; $n = 15$.

TABLE 2. *Change in hemodynamic parameters after maneuvers*

	Basal	Angiotensin	Nitroglycerin
SP	130.60±13.70	201.59±22.82*	137.13±15.35
SD	16.94±1.68	17.59±2.02*	16.99±1.69
DP	79.58±14.65	83.94±15.12	56.72±16.48*
DD	15.19±1.40	15.16±1.59	14.09±1.34*

Values are means ± SD; $n = 15$. SP, systolic pressure (mmHg); SD, systolic diam (mm); DP, diastolic pressure (mmHg); DD, diastolic diam (mm). * $P < 0.05$ with respect to basal state.

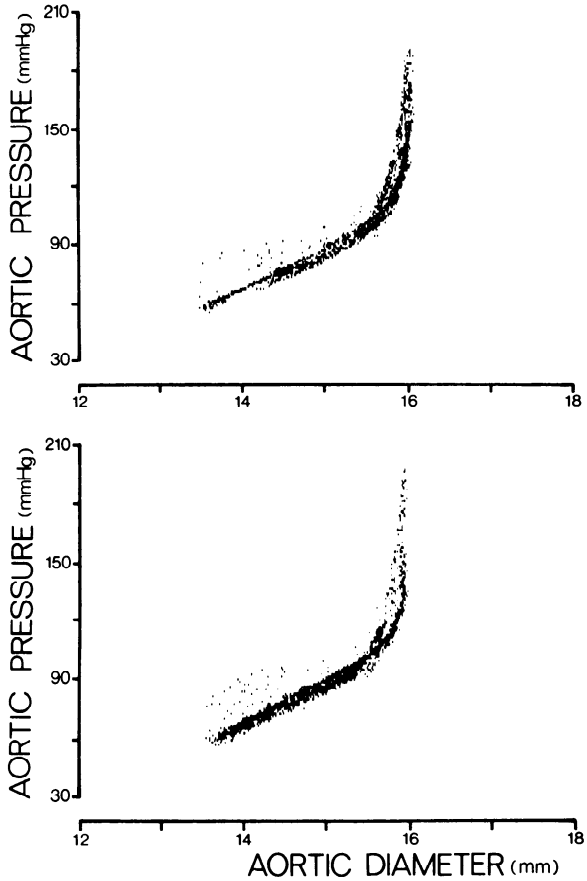

FIG. 4. Aortic pressure-diameter relationship in a typical dog during intravenous angiotensin bolus (*top*) and during occlusion of descending thoracic aorta (*bottom*).

TABLE 3. *Elasticity parameters*

Elasticity Parameters	
E_E, 10^6 dyn/cm^2	4.89±1.72
E_C, 10^6 dyn/cm^2	1,306±637
σ_{BP}, 10^6 dyn/cm^2	1.41±0.43
ϵ_{BP}	1.221±0.063
P_{BP}, mmHg	118.00±16.00
D_{BP}, mm	16.74±1.60
ϵ_{0E}	0.923±0.04
H_m, mm	0.933±0.18
E_P, 10^6 dyn/cm^2	0.669±0.152

Values are means ± SD; $n = 15$. E_E, elastic modulus of elastin fibers; E_C, elastic modulus of collagen fibers; σ_{BP}, stress at breakpoint; ϵ_{BP}, strain at breakpoint; P_{BP}, aortic pressure at breakpoint; D_{BP}, aortic diameter at breakpoint; ϵ_{0E}, strain at zero stress; H_m, mean aortic wall thickness; E_P, pressure-strain modulus.

stress-strain relationships obtained by angiotensin and nitroglycerin boluses.

Table 3 lists the values of the slope (E_E) and intercept (ϵ_{0E}) of the linear regression analysis for the elastin fibers, E_C, and the values of stress, strain, and aortic pressure at the breakpoint. The E_E was 4.89 ± 1.72 × 10^6 dyn/cm^2, and E_C was 1,306 ± 637 × 10^6 dyn/cm^2. The breakpoint of the stress-strain relationships was found at a stress level of 1.41 ± 0.43 × 10^6 dyn/cm^2 corresponding to a strain of 1.221 ± 0.063. The same point in pressure-diameter relationships was found at a pressure of 118 ± 16 mmHg and a diameter of 16.74 ± 1.60 mm. The mean wall thickness of the basal beats was 0.933 ± 0.18 mm, and the E_P was 0.669 ± 0.152 × 10^6 dyn/cm^2.

The variability study is presented in Table 4. Values are the coefficients of variation of each parameter obtained by averaging the results of the three experimental sessions in the four dogs involved in this analysis. Pulse pressure and diameter, and E_C and E_P presented coefficients of variation >10%, whereas E_E and the parameters obtained at breakpoint level showed coefficients of variation <6%. The analysis of the day-to-day repeatability for all the parameters showed no statistical differences between *days 1, 2,* and *3*.

The overall FC as a function of transmural pressure is shown in Fig. 5. The percentage of FC at the pressure level observed at the breakpoint of the stress-strain relationship was 6.09 ± 2.6%. The high day-to-day repeatability of the FC function for a typical dog is shown in Fig. 6.

DISCUSSION

The aim of this study was to develop in conscious, unsedated, chronically instrumented dogs a method for assessing and discriminating E_E and E_C and also for determining the FC at a given level of transmural pres-

TABLE 4. *Coefficients of variation*

	Dog 1	Dog 2	Dog 3	Dog 4	Means ± SD
E_E	8.56	3.56	0.58	7.81	5.128±3.745
E_C	20.58	31.43	26.52	38.56	29.273±7.617
σ_{BP}	2.67	9.69	1.59	6.11	5.017±3.665
ϵ_{BP}	4.52	2.87	2.32	1.69	2.855±1.210
P_{BP}	4.07	8.80	2.93	8.03	5.959±2.891
D_{BP}	2.03	1.59	0.88	1.29	1.448±0.487
ϵ_{0E}	3.20	6.08	2.99	3.47	3.936±1.446
APP	25.33	14.42	5.32	17.18	15.562±8.524
APD	20.03	20.07	11.00	21.82	18.231±4.891
E_P	10.97	17.51	10.51	8.72	11.929±3.844

Values are expressed as coefficients of variation (SD/mean) × 100 from 3 repeated experimental sessions in each dog. E_E, elastic modulus of elastin fibers; E_C, elastic modulus of collagen fibers; σ_{BP}, stress at breakpoint; ϵ_{BP}, strain at breakpoint; P_{BP}, aortic pressure at breakpoint; ϵ_{0E}, strain at 0 stress; APP, aortic pulse pressure; APD, aortic pulse diameter; E_P, pressure-strain elastic modulus.

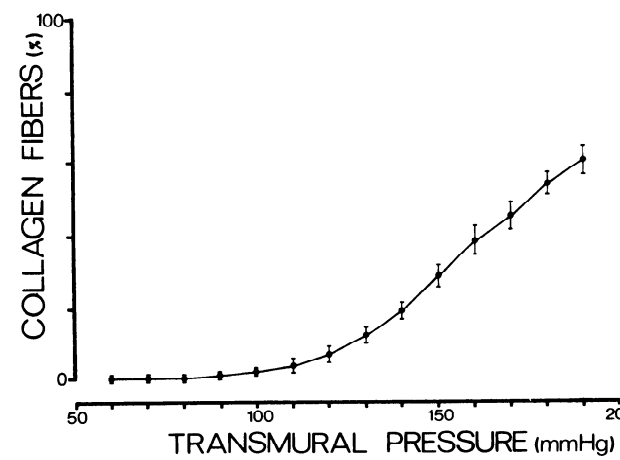

FIG. 5. Recruitment function of collagen fibers as a function of transmural pressure. Each point indicates mean ± SE of %fraction of collagen fibers supporting wall stress at a given level of pressure.

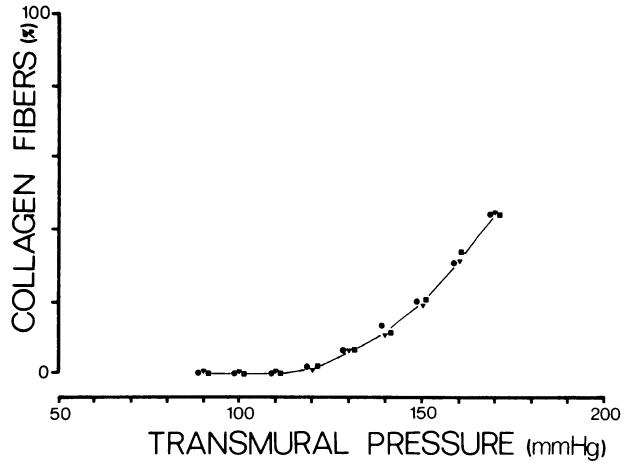

FIG. 6. Repeatability study for a typical dog. Each symbol represents fraction of collagen fibers supporting wall stress at a given level of pressure during 3 different experimental sessions.

sure. The mathematical approach used in this study allows the characterization of the elastic behavior of the arterial wall with single elastic moduli for elastin and collagen. At first we determined the pressure-diameter relationship in the conscious animal using ultrasonic dimension transducers and a miniature pressure gauge (Konigsberg P7) (26, 28, 37). The high-frequency responses of the dimension gauge and the pressure transducer and the linearity of their responses allowed accurate and reproducible measurements over a long period of time. The 200-Hz sampling rate used in the digitalization of the data is at least two times higher than the highest frequency components in the pressure and diameter spectra, thus allowing signal reconstruction without distortion. To study the elastic behavior of individual components, we induced wider variations (Table 2) in pressure and diameter than those occurring spontaneously in the basal state. These variations, obtained by vasoactive drugs or by use of an implanted hydraulic occluder, were virtually identical. This indicates that the drugs using for varying aortic pressure were acting only at the arteriolar level but had no direct action on the aortic wall. This observation is in accordance with the results of Pagani et al. (27) showing that the peak effect of pressure change under drug occurs in <25 s, so that the variations in pressure and diameter in the aorta are extremely rapid and only reflect the intrinsic passive elastic properties of the vessel wall.

The elastic parameters were calculated from aortic diameter and pressure signals previously converted into stress and strain utilizing a thick-walled cylindrical tube model and linear elastic theory. The validity of the use of this theory to describe the aortic mechanical properties as well as the use of a static elastic modulus to study the aortic elastic behavior has been discussed by Pagani et al. (27). On the other hand, the use of conscious animals chronically instrumented to analyze the mechanical properties of the arterial wall have been widely supported (5, 6, 17, 18, 26, 27, 35). Roach and Burton (32) have suggested that the initial slope of the stress-strain relationship may be used to determine the amount of elastin fibers. A more complete description of the passive mechanical properties of the arterial wall was introduced by Cox (9, 11) on the basis of a model assuming that the collagen and elastin fibers are arranged in parallel. To adapt this approach to conscious animals, the present study breaks down the original stress-strain diagram to separate elastin and collagen stress-strain relationships. The stress-strain relationship of elastin has been shown to be almost a straight line (16) and at low strain ranges the resistance to stretch is due to elastin alone (32). For this reason, a linear correlation was used to characterize the elastin stress-strain relationship and evaluate E_E. We then calculated the collagen response by subtracting the elastin stress-strain relationship from the entire relationship at equal levels of strain. The stress-strain locus thus obtained represents the resistance to stretch due to both the stiffness and the recruitment function of the collagen fiber assembly and is revealed by the nonlinear behavior of this relationship (Fig. 3*B*). The final phase of the collagen stress-strain relationship at the highest levels of stress is a linear function due to "unwrinkling" of the collagen fibers. The slope of this function is close to the E_C modulus.

The E_C and E_E values obtained in vivo by using our approach were virtually identical to those found in in vitro preparations (9, 32). In these preparations, E_E has been found to be equal to $2.8 \pm 0.4 \times 10^6$ dyn/cm^2, and E_C was equal to $1{,}200 \pm 100 \times 10^6$ dyn/cm^2. Dobrin (14) reported a value for the elastic modulus of $\sim 4 \times 10^6$ dyn/cm^2 at normal pressure levels in which the participation of elastin fibers plays a major role, whereas at high pressure levels this value rose to 10×10^6 dyn/cm^2, significantly less than that observed in isolated collagen fibers. When our data were analyzed using an exponential fit to characterize the collagen stress-strain relationship, the derivative of this function, which is approximately E_C, was $\sim 10 \times 10^6$ dyn/cm^2 at high levels of stress. This indicates that this fit is unreliable in the final linear phase of the collagen response, because the strain here shows minimal changes. However, when only the last phase of the collagen stress-strain relationship was analyzed, the E_C modulus was $1{,}306 \pm 637 \times 10^6$ dyn/cm^2, very close to the value obtained in in vitro studies (3, 20). The recruitment function shown in Fig. 5 is quite similar to that illustrated by Cox (9) in different canine arteries. Our results show that $6.09 \pm 2.6\%$ of the collagen fibers were "recruited" at a pressure equal to 118 ± 16 mmHg in the breakpoint, which indicates the onset of significant collagen participation in the vessel resistance to deformation. E_P and wall thickness values are close to the values reported in the literature (19, 22, 29). The mean value of aortic pressure at the breakpoint was 118 mmHg, and the systolic arterial pressure was 130.60 mmHg, which means that under control resting conditions, the collagen fibers are almost not distended, and the resistance to stretch is mainly supported by the elastin fibers, i.e., the mechanical behavior of the aorta is almost purely elastic.

The stability of the elastic parameters is very important in the longitudinal evaluation of a single subject. For this reason, we used the coefficient of variation to quantify such variability. Our results showed that in conscious animals E_E and the parameters obtained at the breakpoint had a coefficient of variation <6%, whereas

E_P, pulse pressure, and pulse diameter were >10%. This could be interpreted as being parameter values intrinsic to wall structure that remain constant as long as the arterial wall is not altered. Despite the fact that the E_C showed a variation of ~30%, the mean value of E_C was the parameter that presented the closest similarity to the values reported in the literature. The run to run repeatability for all the parameters was confirmed because no differences were present in the ANOVA for repeated measures.

In the present study, the E_E obtained in vivo is 24.8% greater than that reported by Dobrin (14) from excised vessels and 78.2% greater than that found by Cox (9). These differences might be due to the activation of the smooth muscle tone in conscious animals. Indeed, it is known that the aortic pressure-diameter and stress-strain relationships are affected by the contractile state of the smooth muscle (1, 2, 8, 10, 13–15, 23, 24, 27, 30, 33, 37). The smooth muscle exerts some degree of tension at all times in vivo, and the stiffness that this tension confers to the vessel is the vasomotor tone (4, 24). This active tension can vary greatly in vivo, and there is abundant evidence to indicate that the smooth muscle activation shifts the whole stress-strain relationship toward a higher stress level (2, 8, 13, 14, 23, 27, 33). Studies carried out by Stone and Dujardin (33), analyzing how changes in the smooth muscle tone influence the characteristic impedance of the aorta, found that hemorrhage caused a change in aortic smooth muscle activity that decreased its diameter at a given pressure. They stated that the slope of the pressure-diameter relationship was influenced by changes in the aortic smooth muscle activity. In addition, Pagani et al. (27) obtained a shift toward a higher stress level at a given midwall radius in the stress-strain relationship under methoxamine infusion in conscious adult sheep.

From the results obtained in the present study, we were not able to identify if in vivo E_E represents the mechanical characteristics of both elastic and muscular fibers. Further studies are necessary to demonstrate how the shift in the elastics parameters are quantitatively related to the degree of smooth muscle activation and also to characterize the behavior of the three elastic moduli corresponding to each of the main orthogonal axes (E_R, E_θ, E_Z, radial, circumferential, and longitudinal elastic moduli, respectively) due to the anisotropy of the arterial wall.

In conclusion, this method permits accurate and reliable assessment of E_E and E_C in conscious animals. It also yields FC, which may be of interest in studies of connective tissue disease involving the aortic wall.

This work was supported by grants from an Institut National de la Santé et de la Recherche Médicale-Consejo Nacional de Investigaciones Cientificas y Técricas cooperation agreement and by the Gregorio Pérez Companc Company.

Address for reprint requests: R. Armentano, Teaching and Research Department, Favaloro Foundation, Solís 453, 1078 Buenos Aires, Argentina.

Received 26 December 1989; accepted in final form 31 January 1991.

REFERENCES

1. AARS, H. Diameter and elasticity of the ascending aorta during infusion of noradrenaline. *Acta Physiol. Scand.* 83: 133–138, 1971.
2. BADER, H. Importance of the gerontology of elastic arteries in the development of essential hypertension. *Clin. Physiol. Biochem.* 1: 36–56, 1983.
3. BURTON, A. C. Relation of structure to function of the tissues of the wall of blood vessels. *Physiol. Rev.* 34: 619–642, 1954.
4. BURTON, A. C. *Physiology and Biophysics of the Circulation* (2nd ed.). Chicago, IL: Year Book, 1972, p. 63–75.
5. CABRERA, E. I., J. LEVENSON, R. L. ARMENTANO, J. G. BARRA, R. H. PICHEL, AND A. SIMON. Constricting and stiffening action of atropine on aortic response to angiotensin in dogs. *Hypertension Dallas* 11, *Suppl.* I: I-103–I-107, 1988.
6. CABRERA, E. I., J. LEVENSON, R. L. ARMENTANO, J. G. BARRA, R. H. PICHEL, AND A. SIMON. Aortic pulsatile pressure and diameter response to intravenous perfusions of angiotensin, norepinephrine and epinephrine in conscious dogs. *J. Cardiovasc. Pharmacol.* 12: 643–649, 1988.
7. COX, R. H. Three-dimensional mechanics of arterial segments in vitro: methods. *J. Appl. Physiol.* 36: 381–386, 1974.
8. COX, R. H. Effects of norepinephrine on mechanics of arteries in vitro. *Am. J. Physiol.* 231: 420–425, 1976.
9. COX, R. H. Passive mechanics and connective tissue composition of canine arteries. *Am. J. Physiol.* 234 (*Heart Circ. Physiol.* 3): H533–H541, 1978.
10. COX, R. H. Regional variation of series elasticity in canine arterial smooth muscles. *Am. J. Physiol.* 234 (*Heart Circ. Physiol.* 3): H542–H551, 1978.
11. COX, R. H. Comparison of arterial wall mechanics in normotensive and spontaneously hypertensive rats. *Am. J. Physiol.* 237 (*Heart Circ. Physiol.* 6): H159–H167, 1979.
12. DE FORTEZA, E., R. L. ARMENTANO, M. BIAGETTI, AND E.M. RODRIGUEZ CHATRUC. Real-time pressure-volume diagrams for the evaluation of ventricular function. *J. Biomed. Eng.* 8: 200–205, 1986.
13. DOBRIN, P. B., AND A. A. ROVICK. Influence of vascular smooth muscle on contractile mechanics and elasticity of arteries. *Am. J. Physiol.* 217: 1644–1652, 1969.
14. DOBRIN, P. B. Mechanical behaviour of vascular smooth muscle in cylindrical segments of arteries in vitro. *Ann. Biomed. Eng.* 12: 497–510, 1984.
15. DUJARDIN, J. P., L. T. PAUL, AND H. P. PIEPER. Effect of acute volume loading on aortic smooth muscle activity in intact dogs. *Am. J. Physiol.* 238 (*Heart Circ. Physiol.* 7): H379–H383, 1980.
16. FUNG, Y. C. *Biomechanics.* New York: Springer-Verlag, 1981, p. 196–257.
17. GENTILE, B. J., C. J. CHUONG, AND G. A. ORDWAY. Regional volume distensibility of canine thoracic aorta during moderate treadmill exercise. *Circ. Res.* 63: 1012–1019, 1988.
18. GENTILE, B. J., D. R. GROSS, C. J. CHUONG, AND N. C. H. HWANG. Segmental volume distensibility of the canine thoracic aorta in vivo. *Cardiovasc. Res.* 22: 385–389, 1988.
19. GOW, B. S., AND M. G. TAYLOR. Measurement of viscoelastic properties of arteries in the living dog. *Circ. Res.* 23: 111–122, 1968.
20. LI, J. K.-L. *Arterial System Dynamics.* New York: New York Univ. Press, 1987, p. 6–21.
21. LING, S. C., AND C. H. CHOW. The mechanics of corrugated collagen fibrils in arteries. *J. Biomech.* 10: 71–77, 1977.
22. MCDONALD, D. A. *Blood Flow in Arteries*, (2nd ed.). Baltimore, MD: Williams & Wilkins, 1974.
23. MEGERMAN, J., J. E. HASSON, D. F. WARNOCK, G. J. L'ITALIEN, AND W. M. ABBOTT. Noninvasive measurements of nonlinear arterial elasticity. *Am. J. Physiol.* 250 (*Heart Circ. Physiol.* 19): H181–H188, 1986.
24. MILNOR, W. R. *Hemodynamics* (2nd ed.). Baltimore, MD: Williams & Wilkins, 1982, p. 56–96.
25. O'ROURKE, M. F. *Arterial Function in Health and Disease.* New York: Churchill Livingstone, 1982, p. 153–169.
26. PAGANI, M., H. BAIG, A. SHERMAN, W. T. MANDERS, P. QUINN, T. PATRICK, D. FRANKLIN, AND S. F. VATNER. Measurement of multiple simultaneous small dimensions and study of arterial pressure-dimension relations in conscious animals. *Am. J. Physiol.* 235 (*Heart Circ. Physiol.* 4): H610–H617, 1979.
27. PAGANI, M., I. MIRSKY, H. BIAG, W. T. MANDERS, P. KERKHOF,

AND S. F. VATNER. Effects of age on aortic pressure-diameter and elastic stiffness-stress relationships in unanesthetized sheep. *Circ. Res.* 44: 420–429, 1979.

28. PATRICK, T. A., S. F. VATNER, W. S. KEMPER, AND D. FRANKLIN. Telemetry of left ventricular diameter and pressure measurements from unrestrained animals. *J. Appl. Physiol.* 37: 276–281, 1974.
29. PETERSON, L. H., R. E JENSEN, AND J. PARNELL. Mechanical properties of arteries in vivo. *Circ. Res.* 8: 622–639, 1960.
30. PIEPER, H. P., AND L. T. PAUL. Responses of aortic smooth muscle studied in intact dogs. *Am. J. Physiol.* 217: 154–160, 1969.
31. PRICE, J. M. Length-dependent activation and sensibility in arterial ring segments. *Ann. Biomed. Eng.* 12: 481–496, 1984.
32. ROACH, M. R., AND A. C. BURTON. The reason for the shape of the distensibility curves of arteries. *Can. J. Biochem.* 35: 681–690, 1957.
33. STONE, D. N., AND J. P. L. DUJARDIN. Changes in smooth muscle tone influence characteristic impedance of the aorta. *Am. J. Physiol* 246 (*Heart Circ. Physiol.* 15): H1–H7, 1984.
34. VAISHNAV, R. N., J. T. YOUNG, J. S. JANICKI, AND D. J. PATEL. Nonlinear anisotropic elastic properties of the canine aorta. *Biophys. J.* 12: 1008–1027, 1972.
35. VATNER, S. F., A. PASIPOULARIDES, AND I. MIRSKY. Measurement of arterial pressure-dimension relationships in conscious animals. *Ann. Biomed. Eng.* 12: 521–534, 1984.
36. WINER, B. J. *Statistical Principles in Experimental Design* (2nd ed.). New York: McGraw-Hill, 1962.
37. YANO, M., T. KUMADA, M. MATSUZAKI, M. KOHNO, T. HIRO, S. KOHTOKU, T. MIURA, K. KATAYAMA, M. OZAKI, AND R. KUSUKAWA. Effect of diltiazem on aortic pressure-diameter relationship in dogs. *Am. J. Physiol.* 256 (*Heart Circ. Physiol.* 25): H1580–H1587, 1989.